Emerging mutations in envelope protein of SARS-CoV-2 and their effect on thermodynamic properties

Kejie Mou [a,1], Mohnad Abdalla [b,1], Dong Qing Wei [c,d], Muhammad Tahir Khan [e,*],
Madeeha Shahzad Lodhi [e], Doaa B. Darwish [f], Mohamed Sharaf [g,h], Xudong Tu [i,**]

[a] Department of Neurosurgery, Bishan Hospital of Chongqing, Chongqing, China
[b] Key Laboratory of Chemical Biology (Ministry of Education), Department of Pharmaceutics, School of Pharmaceutical Sciences, Cheeloo College of Medicine, Shandong University, 44 Cultural West Road, Shandong Province, 250012, PR China
[c] State Key Laboratory of Microbial Metabolism, Shanghai-Islamabad-Belgrade Joint Innovation Center on Antibacterial Resistances, Joint International Research Laboratory of Metabolic & Developmental Sciences and School of Life Sciences and Biotechnology, Shanghai Jiao Tong University, Shanghai, 200030, PR China
[d] Peng Cheng Laboratory, Vanke Cloud City Phase I Building 8, Xili Street, Nashan District, Shenzhen, Guangdong, 518055, PR China
[e] Institute of Molecular Biology and Biotechnology (IMBB), The University of Lahore, KM Defence Road, Lahore, Pakistan, 58810
[f] Department of Biology, Faculty of Science, University of Tabuk, 71491, Saudi Arabia
[g] Department of Biochemistry and Molecular Biology, College of Marine Life Sciences, Ocean University of China, Qingdao, 266003, PR China
[h] Department of Biochemistry, Faculty of Agriculture, AL-Azhar University, Nasr City, Cairo, 11751, Egypt
[i] Chongqing Medical and Pharmaceutical College, Chongqing, China

ABSTRACT

Structural proteins of severe acute respiratory syndrome coronavirus 2 (SARS-CoV-2) are potential drug targets due to their role in the virus life cycle. The envelope (E) protein is one of the structural proteins; plays a critical role in virulency. However, the emergence of mutations oftenly leads to drug resistance and may also play a vital role in virus stabilization and evolution. In this study, we aimed to identify mutations in E proteins that affect the protein stability. About 0.3 million complete whole genome sequences were analyzed to screen mutations in E protein. All these mutations were subjected to stability prediction using the DynaMut server. The most common mutations that were detected at the C-terminal domain, Ser68Phe, Pro71Ser, and Leu73Phe, were examined through molecular dynamics (MD) simulations for a 100ns period. The sequence analysis shows the existence of 259 mutations in E protein. Interestingly, 16 of them were detected in the DFLV amino acid (aa) motif (aa72-aa75) that binds the host PALS1 protein. The results of root mean square deviation, fluctuations, radius of gyration, and free energy landscape show that Ser68Phe, Pro71Ser, and Leu73Phe are exhibiting a more stabilizing effect. However, a more comprehensive experimental study may be required to see the effect on virus pathogenicity. Potential antiviral drugs, and vaccines may be developed used after screening the genomic variations for better management of SARS-CoV-2 infections.

1. Introduction

Recently the newly emerged coronavirus disease-19 (COVID-19) remains a major public health issue since 2019. The causative agent severe acute respiratory syndrome coronavirus 2 (SARS-CoV-2) [1] is passing through numerous evolutionary stages [2,3] and seems more

fatal. The virus is rapidly spreading through respiratory droplets, affecting the important organs of the host body [2,3].

Since the coronavirus 2 (CoV-2) belongs to the formerly known family of coronaviruses, it shares close genomic similarity with SARS-CoV. The CoV-2 contains the ssRNA genome [6]; it encodes four structural proteins such as a spike (S), an envelope (E), membrane (M), and
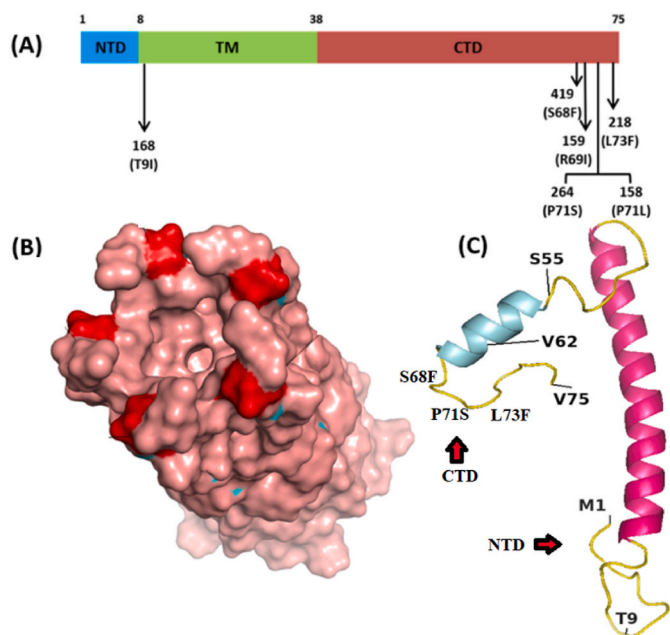
Fig. 1. Domain organization of E proteins and the location and frequency of most common mutations. TM: transmembrane [15], NTD: N-terminal domain, CTD: C-terminal domain. (B). Pentameric representation of E proteins showing channel (C). Full-length E protein (I-TASSER, E-QHD43418) with most common mutations in the loop region.

Table 1
Frequency of some common mutations in the CoV-2 E protein.

Accession	Wild type AA	Position	Mutated AA	Frequency	[a]Mutation
EPI_ISL_476911	T	9	I	168	T9I
EPI_ISL_424214	S	55	F	128	S55F
EPI_ISL_538676	V	62	F	129	V62F
EPI_ISL_448073	S	68	F	[b]419	[b]S68F
EPI_ISL_452908	R	69	I	159	R69I
EPI_ISL_577907	P	71	L	158	P71L
EPI_ISL_660339	P	71	S	[b]264	[b]P71S
EPI_ISL_478788	L	73	F	[b]218	[b]L73F

[a] Full list is available in the S1 supplementary file.
[b] ; mutations subjected to MD simulations.

nucleocapsid (N) [7], resulting in the coding of 16 non-structural proteins (NSPs). These structural proteins are responsible for viral replication and virion-receptor attachments and, thus, are involved in pathogenicity, viral spread, and the introduction of the virus to the cells of the host body.

The E protein is composed of 76 amino acids [8] weighing 8–12 kDa [9]. This protein has an N-terminal domain (NTD), hydrophobic domain, and C-terminal domain (CTD) [10], arranged as NTD first 1–9 amino acid (aa), the hydrophobic area, extending from 10 to 37 aa and CTD (38–75 aa) [11]. Ionic pores are formed across the membrane due to the arrangement of the hydrophobic tail region. Structurally, the E protein consists of seven alpha helices and eight loop regions. It forms a pentameric configuration (five molecules) with 35 alpha-helical regions and 40 looped ring regions, which are formed by the hydrophobic tail (Fig. 1B). This pentameric configuration of the hydrophobic tail can be affected by the interactions within CTD [12]. These pores serve as ion channels that allow the movement of the virus across the membrane, enhancing its pathogenicity [13]. E mutations reduce viral pathogenicity and also stop the channel activity [14] representing an essential drug target and vaccine candidate [15].

Some novel mutations seen in the E protein sequence do not present in the already existing coronaviruses. In the CoV-2 E protein sequence, arginine is mutated by isoleucine, threonine, and lysine (R69I, R69T, and R69K) at the 69th position. Moreover, in the amino acid sequence of CoV-2, serine and phenylalanine are present at 55th and 56th positions, instead of threonine and valine, respectively [16].

The SARS-CoV-2 has undergone numerous mutations in all the important targets [17–19]; therefore, drugs created to fight CoV-2 might not very potent. In order to evaluate the drug targets for designing novel antiviral drugs against CoV-2, it is vital to screen the frequency of mutations and their effect on the thermodynamic properties of the important target proteins. This is particularly important for the effective treatment of emerging microbes, including mutants of SARS-CoV-2.

Although structural proteins of CoV-2 are important for investigating mutations, here in this study, we investigated the variations existing only in E proteins owing to their potential drug target. Very limited information and small-scale genomic data has been screened for mutations in the E protein. This is the first comprehensive study in which we screened 0.295 million complete genomes of SARS-CoV-2 for identifying variants in the E protein. Among all the genomes, 259 mutations were detected, exhibiting various degrees of thermodynamic properties.

Analyzing the frequency of mutations and their effect on the thermodynamics properties of E proteins may allow the researcher to design novel inhibitors and predict the level of pathogenicity and transmission. In the current study, the most common mutations that were detected at
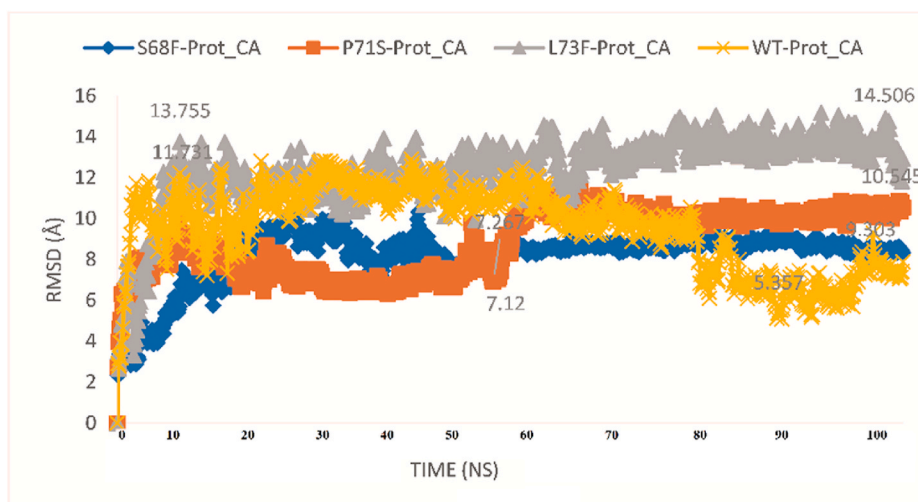

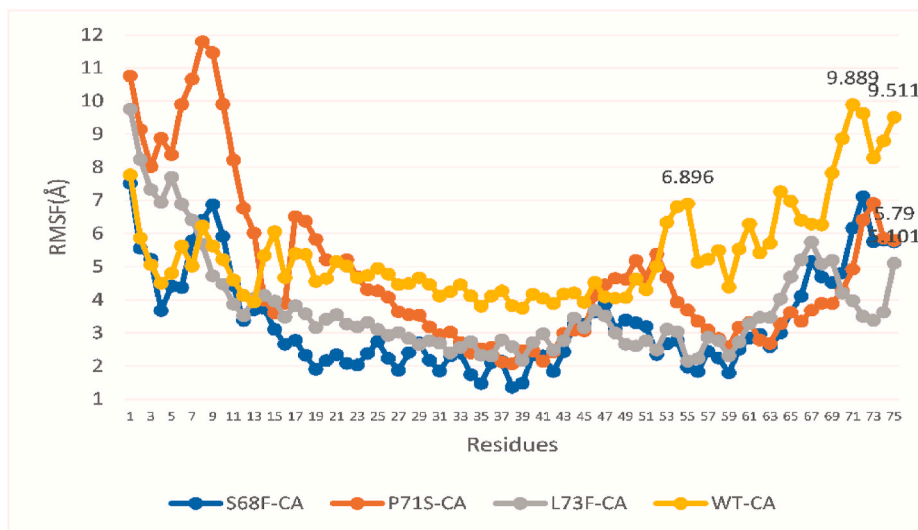**Fig. 2.** RMSD comparison of the WT and MTs E proteins of SARS-CoV-2.

Fig. 3. The RMSF of the WT and MTs in the E proteins of SARS-COV-2. CA: Carbon alpha. The RMSF of WT (orange) and MTs. (For interpretation of the references to color in this figure legend, the reader is referred to the Web version of this article.)
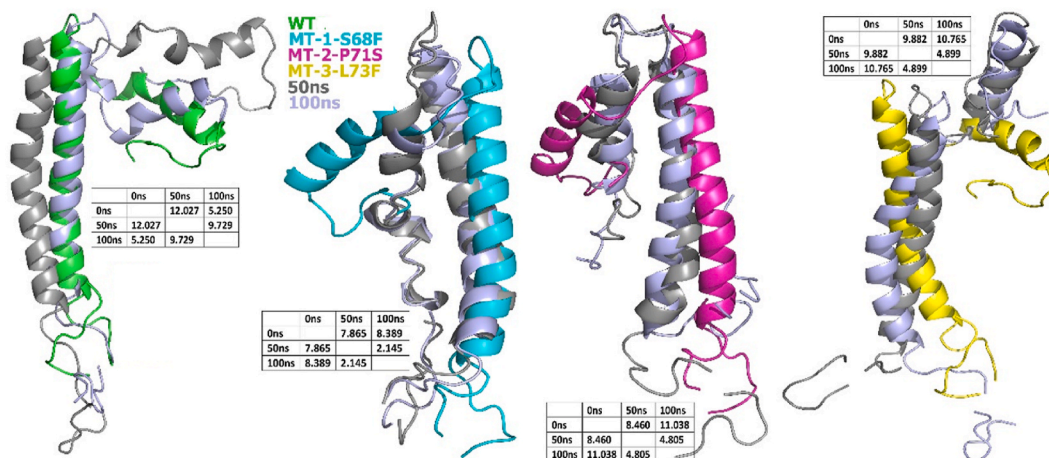

Fig. 4. The RMSDs of WT and MTs at different simulation periods. The WT behaves very differently at the CTD.

the C-terminal (Ser68Phe, Pro71Ser, Leu73Phe) were exhibiting more stabilizing effect on E proteins structure. First, the presence of a large number of mutations in the E protein of CoV-2 may lead to the conformational changes and evolutions, resulting in therapeutic failure. Secondly, the virus may be more fatal in near future, and therefore, antivirals against geography-specific CoV-2 strains might be more effective.

2. Methodology

2.1. Genomic sequence retrieval

The complete genome was retrieved from the Global Science Initiative on Sharing All Influenza Data (GISAID) (December 2019–2020) (https://www.gisaid.org/) [20]. The GISAID shared the virus data to publish results and the metadata relevant to public health scientists. This server provides all kinds of CoV-2 genomic data, including even those that have not been unpublished. We screened 0.295 genomes of CoV-2 reported worldwide for variants analysis in E proteins. The sequences were aligned with the reference CoV-2 genome (Accession NC_045512) using the CoVsurver application (https://www.gisaid.org/epiflu-appl ications/covsurver-mutations-app/). The identified mutations in structural proteins of CoV-2 were separated and arranged in the form of excel

sheets. The statistical analysis was performed to screen the most common variants.

2.2. Structural information

Scientists are all well aware that sharing the genomic and proteomic data of SARS-CoV-2 is important for the better management of infectious diseases in order to devise countermeasures. The E protein structural data was retrieved from the protein data bank (PDB) [21] (PDB IDs: E = 7k3g). Some residues at the NTD (1–7aa) and CTD (39–75) are missing in the PDB structure of the COV-2 E protein. To observe the effect of mutations on the residues missing in the CTD and ND terminals, the full-length E protein structure was downloaded (E-QHD43418) from I-TASSER [22,23]. The chain ID in the I-TASSER structure is missing, which was added in PYMOL using the code "sele, chain'" and "alter (sele), chain = 'A'." The I-TASSER has already modeled the full-length proteins of CoV-2 using the NCBI reference data (NC_045512) (GenBank MN908947).

2.3. Mutation effect on E proteins' dynamic stability

All the observed mutations were recorded and their effect on the E protein structure was computed using the DynaMut [24]. The server
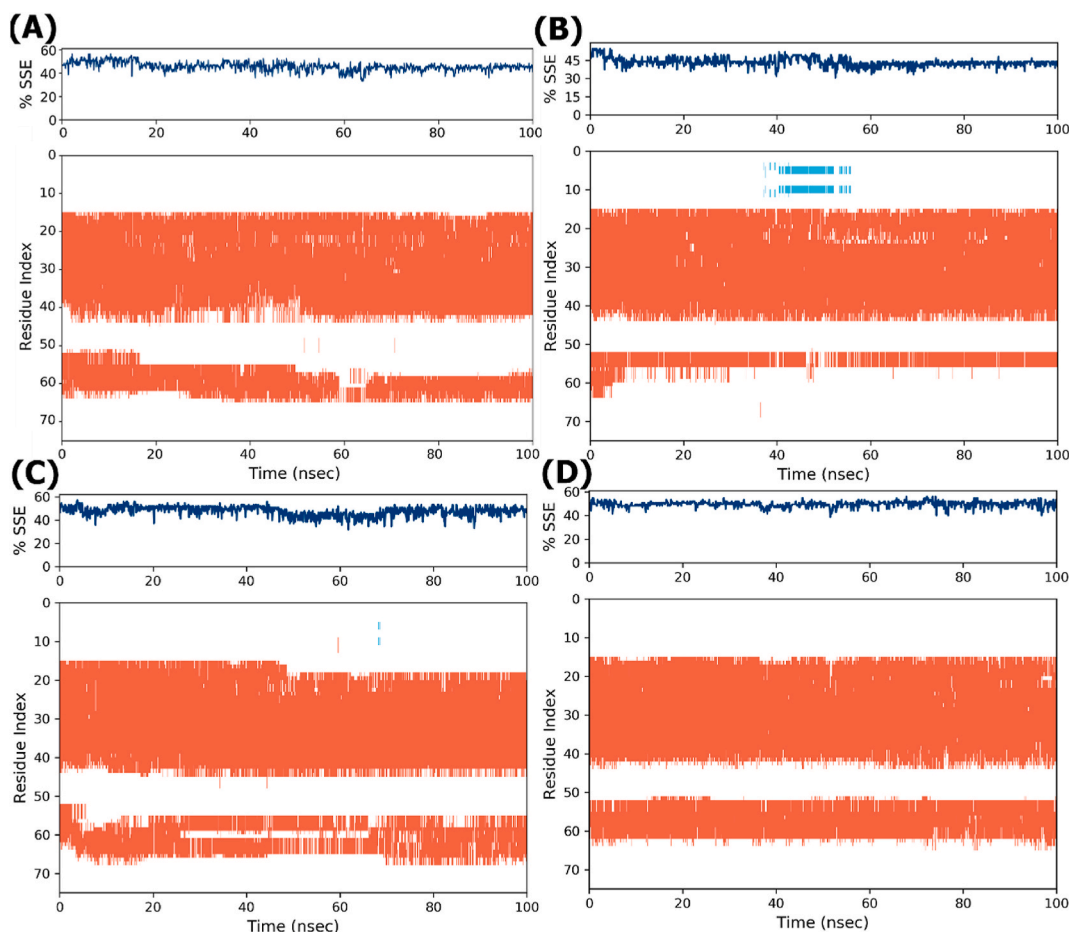
Fig. 5. Comparison of the SSE of the WT and MTs in MD simulation. The plot reports SSE distribution by residue index throughout the protein structure and summarizes the SSE composition for each trajectory frame over the course of the simulation. The plot monitors each residue and its SSE assignment over a certain period of time. (A) The WT residue index and SSE along Y-axis shows differences at the 60–65ns MD simulations period; (B) S68F shows a little variation at 40–55ns; (C) P71S exhibits more variations at 45–68ns; (D) L73F also demonstrates variations when the WT is compared with P71S and S68F.
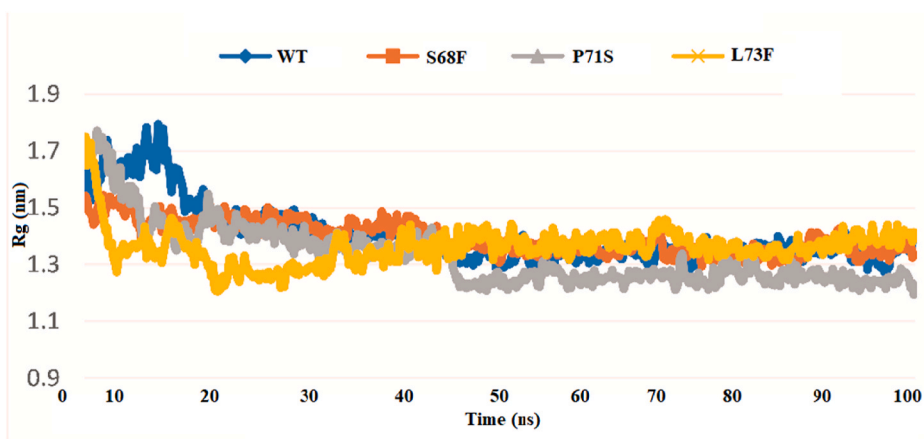
Fig. 6. Comparison of Rg of the WT and MTs E proteins. The WT (blue) exhibited a little difference in folding throughout the 100ns simulation period as compared to the MTs, showing that the folding in both types is stable. (For interpretation of the references to color in this figure legend, the reader is referred to the Web version of this article.)

implemented the mutation effect and also the normal mode methods that can be used to analyze the variants that affect protein stability and flexibility. This impact is measured through graph-based signatures and also as a normal mode. This method outperforming (P < 0.001) with results are also displayed in good resolution.

2.4. Molecular dynamics (MD) simulation

The MD simulation was performed on the Desmond module (Schrodinger), as described in the previous study [23,24]. Briefly, the TIP3P model and Gromos9643a1 forefield was applied. The system was neutralized with counterions (NaCl). The cubic simple point charge

Fig. 7. Hydrogen bonding of the WT and MTs E proteins.

Fig. 8. WT and MTs stability and flexibility.

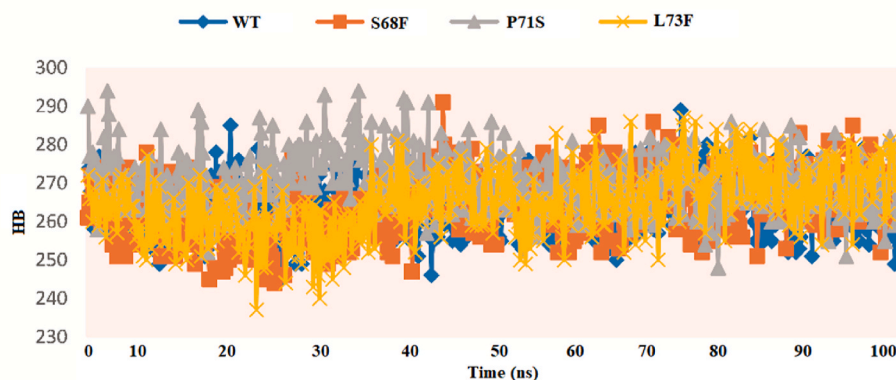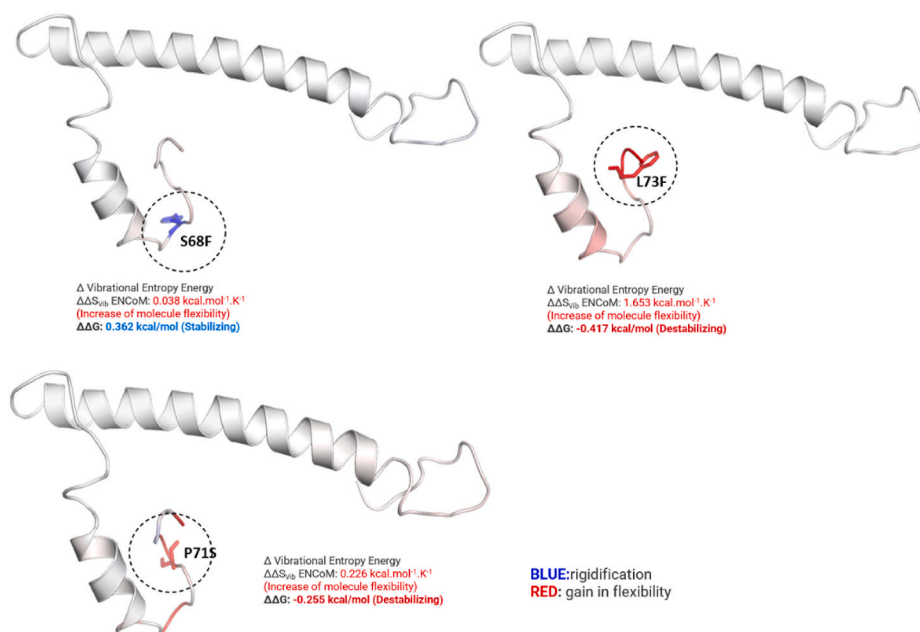(SPC) water box was applied. Two-step (NVT and NPT) energy minimization (50000 ps) till the minimization completion was continued. The ambient pressure was set at 1.013 bar and temperature 310 K for 100 ns? The thermodynamic stability of the WT (wild type) and mutants (MT) E proteins was analyzed using root means square fluctuations (RMSF) and root means square deviation (RMSD). All the simulation were repeated three time for better results. Approximately 1000 frame per simulation was run.

2.5. The Gibbs free energy

The Gibbs free energy (G) [27] of MTs was plotted against wild type E protein. The G is minimized to equilibrium state of system at constant temperature and pressure which is a thermodynamic potential. Principal component analysis (PCA) is performed to recognize low modes in proteins [28,29]. PCA simplifies the complicated motion in trajectory [30–32]. A set z1, z2 …, zp known as principal components (PCs) were generated during PCA. Energies of sets of proteins conformations is called Free Energy Landscape (FEL) [33,34]. The first two components (PC1 and PC2) give the trajectories on initial two principal components of motion. G values shows the stability level of proteins [35–37].

3. Results and discussion

This is the first comprehensive study in which 0.295 million complete genomic sequences of CoV-2, which were reported worldwide in the GISAID server (from December 2019 to December 2020), were analyzed to identify variants in E proteins. A large number of non-synonymous mutations (259) were detected in the genome sequences from 48 countries (Supplementary Table S1), among which the largest number were present in isolates from England (S1). This wide range of variations may project the variation level of CoV-2 strains worldwide. Previous studies [25,26] have screened 3617 and 81,818 COV-2 genomes for E protein variants, respectively. These recent studies reported 115 and 15 non-synonymous mutations, respectively, which were mainly present in the CTD.

3.1. Mutations in envelope (E) protein

3.1.1. Mutations in the NTD

Being the smallest structural protein (75aa) of CoV-2, all of the residues' positions of the E protein harbored non-synonymous mutations (S1). A total of 31 non-synonymous mutations were detected in the NTD
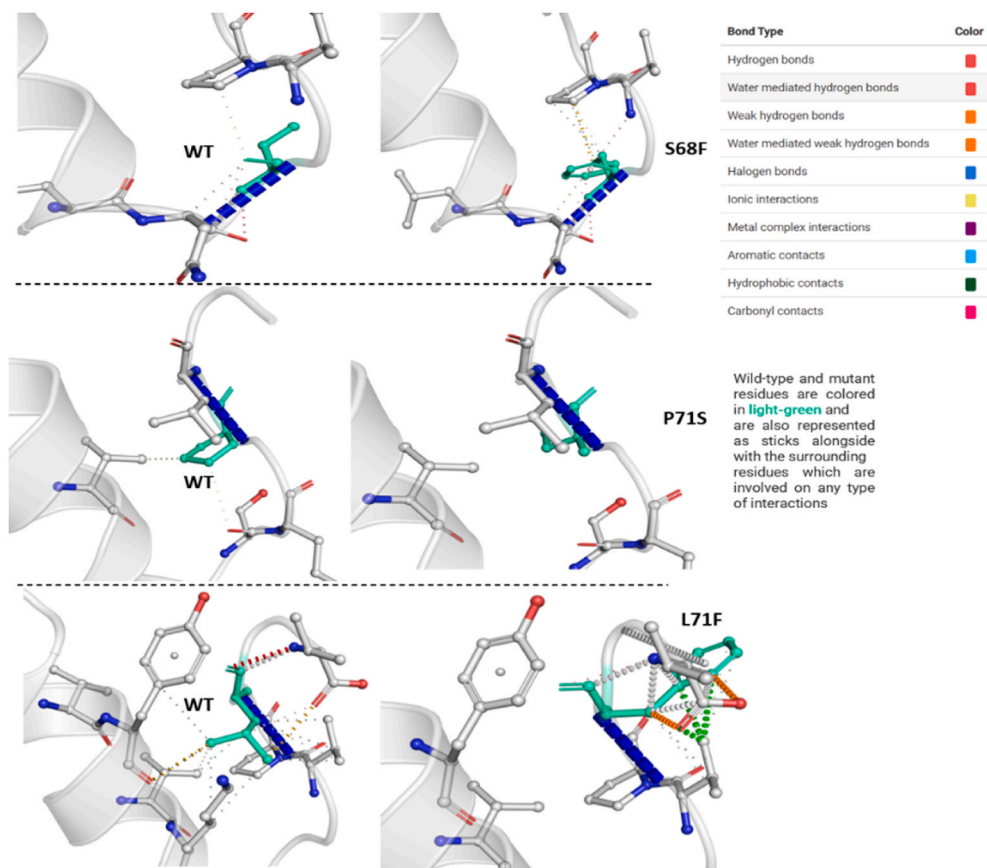
Fig. 9. Interactions of WT and MTs residues with surrounding aa. The type of interactions of WT and MTs residues is colored-coded. S68F, P71S, and L73F MTs have been compared with their WT on the left.

(Supplementary File S1), among which V5F (n = 39), E8D (n = 35), V5I (n = 17), and Y2H (n = 14) were common. A majority of these mutations were detected in the isolates from the UK. The NTD helps the tail region target the Golgi complex using some of its associated elements as mutations in this region may affect its efficiency.

3.1.2. Mutations in the CTD

The most frequent mutations were detected in the CTD of the E protein (68–73 aa) (Table 1). Some of them were T91, S55F, V62F, S68F, R691, P71L, P71S, and L73F (Fig. 1). Other common mutations have been listed in the table along with their residue types and positions (Table 1 and S1). Mutations in the CTD, namely, S55F (128), V62F (129), and R69I (159) may affect the virus pathogenesis, altering the binding of the E protein to a tight junction. The motif "DLLV" (72–75 aa) of the CTD showed some mutations that may affect the PALS1 (Protein Associated with *Caenorhabditis elegans* Lin-7 protein 1) at the Golgi complex, as well as CoV-2 infectivity [38,40]. The PALS1 is a member of the post-synaptic density protein-95/Discs Large/Zonula occludens-1 (PDZ) domain-containing proteins group that is involved in diverse cellular functions and also functions as scaffolds for signaling protein [28,29].

3.1.3. Mutations in the transmembrane (TM) domain

Transmembrane variants such T9I (n = 168), F20L (n = 90), L21F (n = 84), V24 M (n = 76), and T30I (n = 72) may affect the homo pentameric configuration of the E protein [43]. The E protein may also be an effective drug target as it contributes equally to the pathogenicity and cytotoxicity of the virus. It produces viroporins that are hydrophobic in nature [44]. Proline residues facilitate the targeting of the cis-Golgi complex by the hydrophobic tail present in the cytoplasm. The release

of these virion particles is facilitated by the ionic gradient present in the endoplasmic reticulum and Golgi compartment through the E protein [8]. Studies on E mutants for highlighting the structural changes of the ion-channel activity behind mutations, might be very helpful for better management of COVID-19.

The CTD of E proteins harbored some common mutations whose stability was predicted. The DynaMut prediction outcome of L73F ($\Delta\Delta$G: −0.417 kcal/mol), P71S ($\Delta\Delta$G: −0.255 kcal/mol) exert a destabilizing effect. However, T9I ($\Delta\Delta$G: 0.190 kcal/mol), P71L ($\Delta\Delta$G: 0.012 kcal/mol), and S68F ($\Delta\Delta$G: 0.362 kcal/mol) shows a stabilizing effect (Supplementary File S1). The most common mutations were detected at the C-terminal (Ser68Phe, Pro71Ser, and Leu73Phe) were also assessed through MD simulations, exerting a stabilizing effect on the E protein of CoV-2.

3.2. Thermodynamic properties

We analyzed the thermodynamic properties of most common variants (Ser68Phe, Pro71Ser, and Leu73Phe) present in the CTD in relation to the E structure stability in comparison with the wild type (WT).

3.2.1. RMSD and RMSF of WT and MTs

The RMSD graphs of then WT and MTs E proteins are shown in Fig. 2. The MTs S68F and P71S seem more stable from 55ns to 100 ns, exhibiting 9 Å and 10.5 Å RMSDs, respectively. The RMSD of the WT still exhibiting fluctuations at 100 ns? Similar to the other MTs, L73F is also exhibiting stable deviations through the simulation period, with 13.7 Å to 14.5 Å RMSD. The WT exhibited 5.3 Å RMSD at the 80ns–95ns period and still seems to rise from 95ns to 100 ns?

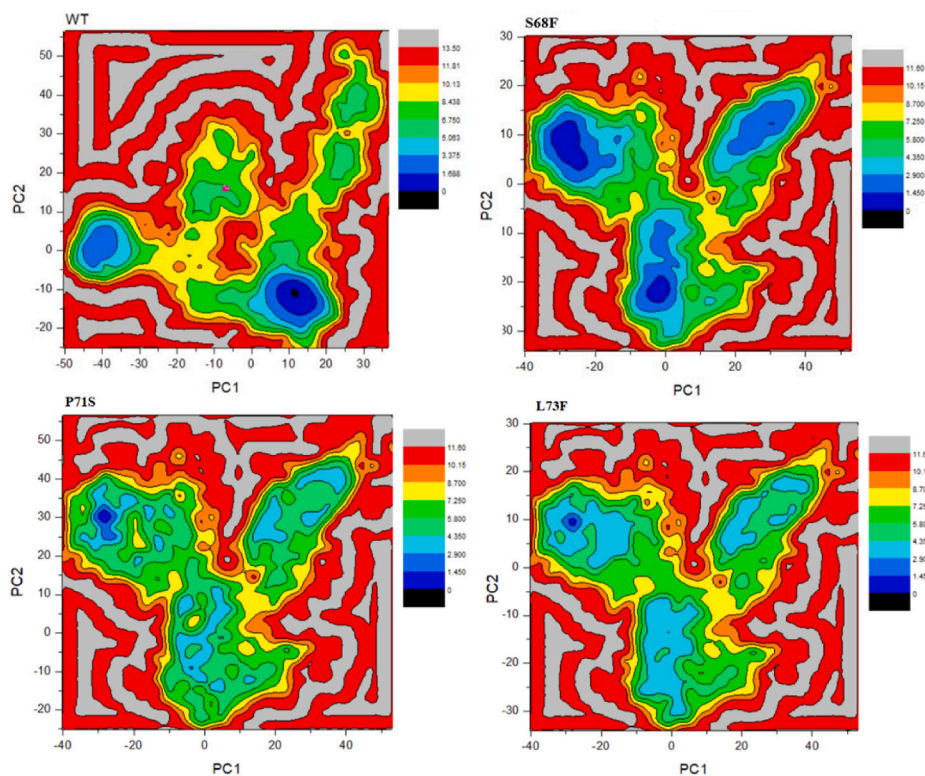The comparison of the WT and MTs in terms of flexibility exhibited

Fig. 10. Gibbs free energy landscape. The scale shows the free energy values. Blue and green regions are more stable than red and yellow. MT S68F shows more stability than WT based on the free energy landscape. WT exhibited more stability than P71S and L73F. (For interpretation of the references to color in this figure legend, the reader is referred to the Web version of this article.)

significant variations at some positions (Figs. 3 and 4). The RMSF at the 53rd to 75th aa position exhibited a significant difference between the WT and MTs. The WTs at this position exhibited 6.89 Å (55 aa), 9.88 Å (71 aa), and 9.5 Å (75 aa); S68F demonstrated very low RMSF, below 4 Å, for the majority of the residues and 5.1 Å at 75 aa, which was significantly low as compared to the WT. Similarly, P71S also exhibited very low RMSF at CTD (5.7 Å) when compared to the WT (Fig. 3). Similar to S68F, the MT L73F also demonstrated low-level fluctuation when compared with the WT. MD simulations explore the insight dynamic changes at the molecular level [45–47], which might be difficult to accomplish through experimental work. Several studies have reported that any change in protein functions might be associated with RMSF [48–50]. Flexibility is one of the key thermodynamic characteristics that maintain the optimal functions of proteins [51]. A large change in this property may alter the function of the biomolecules.

Protein secondary structure elements (SSE) such as alpha helices and beta strands are monitored throughout the simulation. The difference in the SSE of the WT and MTs has been highlighted in Fig. 5 at 20ns–70 ns? The mutation induced some changes in the SSE within a 100ns simulation period. Upon examining Fig. 5, some differences in the SSE of the WT (Fig. 5A) and MTs (Fig. 5B, C, D) can be seen.

3.2.2. Rg of WT and MTs

The degree of protein-folding stability could be measured through Rg. Fluctuations in Rg for a period indicate unstable folding, while a straight value reveals stable folding [52–55]. A protein with misfolding shows variations in Rg over time (Fig. 6). The WT and MTs exhibited variations in folding. The MT S68F exhibited more stable folding than the WT, whereas P71S and L73F also presented stable folding for the 18.9–50ns period (Fig. 6). The S68F MT shows the lowest fluctuations from 21ns to 100 ns (1.3 nm). Rg is a mass-weight root mean square distance between atoms and their common center of mass. It is a vital parameter for defining dynamic stability, offering an insight mechanism

of dimension and compactness of biomolecules and total protein systems. The Rg plotted for three MTs of the CoV-2 E proteins shows notable stability than that of the WT. The mutant structures show a slightly low average Rg value than the WT.

3.2.3. Hydrogen bonding of the WT and the MTs

Most of the interactions among the atoms are mainly hydrogen bonding (HB), which assists in protein folding, stability, and is also involved in recognition. The α helix and β sheet stabilize by the HB potential between the amide nitrogen of the protein and the carbonyl oxygen of the main chain [56–58]. The primary forces in protein–drug interactions are HB, van der Waals, and electrostatic forces [51]. The average number of HB among the WT and MTs CoV-2 E protein atoms is shown in Fig. 7. MT S68F exhibited fewer HB than P71S and P73F. However, both the MTs (P71S and P73F) demonstrated more HB than the WT (Fig. 7), signifying the stabilizing effect of the mutation. P71S exhibited maximum HB (295) during the first 25ns simulations. However, the number of HB in the MD simulation in the last 25ns is almost the same for the WT and MTs.

The effect of mutations on E proteins' stability and flexibility has been shown in Fig. 8. All of the MTs exhibited an increase in flexibility, which may have a positive effect on function. The molecular activities are linked with the flexible regions. According to a previous investigation [59], protein requires flexibility to engage in good catalytic activity. Adding water improves flexibility, and understanding the diverse role of protein flexibility can help develop biotechnological solutions including vaccines.

MTs showed more interactions than WT. The S68F exhibited a different geometry due to the aromatic nature of phenylalanine substitutions. Moreover, the number of interactions in this MT seems greater than in the WT (Fig. 9). In MT P71S, the proline has been substituted into serine, present in the active site of many enzymes. Similar to the S68F, the L73F exhibited more interactions (Fig. 9) with

surrounding residues than the WT due to its substitution into aromatic amino acid, forming more hydrogen interactions with its surrounding residues that might be instrumental in E stability.

The FEL of WT and MTs has been shown in Fig. 10. The lowest and stable energy state is represented by blue color. WT E protein showed more stable state that two MTs (P71S, L73F) whereas the MT S68F seems more stable than WT. The blue areas show stability while other indicate transitions in the protein conformation to attain a more favorable state. The green areas in P71S, L73F are more prevalent that WT which shows stability next to blue regions. These result demonstrates that E protein MTs might be useful to cause viral pathogenecity [60–62]. Calculating G might be important to observe the overall stability upon mutations.

4. Conclusion

In this comprehensive study, 259 non-synonymous mutations were detected in the E protein with different frequencies. Mutations were present in all three domains—the CTD, the NTD, and the hydrophobic domain; however, the highest frequency was detected in the first one. All of the MTs demonstrated various degrees of flexibilities and stabilities, where the majority depicted a loss in flexibility and stability. Moreover, three MTs (S68F, P71S, and L73F) were analyzed through MD simulations and exhibited a stabilizing effect on the E protein structure. In order to evaluate the drug targets for designing a novel antiviral drug against CoV-2, it is vital to dig out the frequency of mutations and their effect on the thermodynamic properties of the selected target. This is particularly imperative for the effective treatment of emerging microbes including SARS-CoV-2 mutants. The current study will contribute significantly to the knowledge on virus stabilization and the evolutionary aspects and pathogenicity of CoV-2 infections, which might be useful for better management of COVID-19 and the development of a vaccine in the near future.

Declaration of competing interest

All the authors have no competing interests.

Appendix A. Supplementary data

Supplementary data to this article can be found online at https://doi.org/10.1016/j.imu.2021.100675.

Author's contribution

Conception and design of the study: XT, MTK, DQW.
Acquisition of data: MTK, XT.
Analysis and interpretation of data: MSL, KM, MTK.
Drafting the article: MTK, MA, KM, DBA.
Revising content: XT, KM, MSL.
Final approval of the version: KM, XT, DQW.

References

[1] Satarker S, Nampoothiri M. Structural proteins in severe acute respiratory syndrome coronavirus-2. Arch Med Res 2020;51:482–91. https://doi.org/10.1016/j.arcmed.2020.05.012.

[2] Banoun H. Evolution of SARS-CoV-2: review of mutations, role of the host immune system. Nephron 2021;145:392–403. https://doi.org/10.1159/000515417.

[3] Rochman ND, Wolf YI, Faure G, Mutz P, Zhang F, Koonin EV. Ongoing global and regional adaptive evolution of SARS-CoV-2. Proc Natl Acad Sci Unit States Am 2021;118. https://doi.org/10.1073/pnas.2104241118.

[6] Naqvi AAT, Fatima K, Mohammad T, Fatima U, Singh IK, Singh A, et al. Insights into SARS-CoV-2 genome, structure, evolution, pathogenesis and therapies: structural genomics approach. Biochim Biophys Acta BBA - Mol Basis Dis 2020;1866:165878. https://doi.org/10.1016/j.bbadis.2020.165878.

[7] Khan A, Tahir Khan M, Saleem S, Junaid M, Ali A, Shujait Ali S, et al. Structural insights into the mechanism of RNA recognition by the N-terminal RNA-binding domain of the SARS-CoV-2 nucleocapsid phosphoprotein. Comput Struct Biotechnol J 2020;18:2174–84. https://doi.org/10.1016/j.csbj.2020.08.006.

[8] Liu DX, Yuan Q, Liao Y. Coronavirus envelope protein: a small membrane protein with multiple functions. Cell Mol Life Sci 2007;64:2043–8. https://doi.org/10.1007/s00018-007-7103-1.

[9] Fung TS, Liu DX. Post-translational modifications of coronavirus proteins: roles and function. Future Virol 2018;13:405–30. https://doi.org/10.2217/fvl-2018-0008.

[10] Ruch TR, Machamer CE. The hydrophobic domain of infectious bronchitis virus E protein alters the host secretory pathway and is important for release of infectious virus. J Virol 2011;85:675–85. https://doi.org/10.1128/JVI.01570-10.

[11] Verdiá-Báguena C, Nieto-Torres JL, Alcaraz A, DeDiego ML, Enjuanes L, Aguilella VM. Analysis of SARS-CoV E protein ion channel activity by tuning the protein and lipid charge. Biochim Biophys Acta BBA - Biomembr 2013;1828:2026–31. https://doi.org/10.1016/j.bbamem.2013.05.008.

[12] Surya W, Li Y, Torres J. Structural model of the SARS coronavirus E channel in LMPG micelles. Biochim Biophys Acta BBA - Biomembr 2018;1860:1309–17. https://doi.org/10.1016/j.bbamem.2018.02.017.

[13] Gupta MK, Vemula S, Donde R, Gouda G, Behera L, Vadde R. In-silico approaches to detect inhibitors of the human severe acute respiratory syndrome coronavirus envelope protein ion channel. J Biomol Struct Dyn 2020:1–11. https://doi.org/10.1080/07391102.2020.1751300.

[14] Nieto-Torres JL, DeDiego ML, Verdiá-Báguena C, Jimenez-Guardeño JM, Regla-Nava JA, Fernandez-Delgado R, et al. Severe acute respiratory syndrome coronavirus envelope protein ion channel activity promotes virus fitness and pathogenesis. PLoS Pathog 2014;10:e1004077. https://doi.org/10.1371/journal.ppat.1004077.

[15] Mandala VS. Structure and drug binding of the SARS-CoV-2 envelope protein transmembrane domain in lipid bilayers. Mol Biol 2020;27:24.

[16] Bianchi M, Benvenuto D, Giovanetti M, Angeletti S, Ciccozzi M, Pascarella S. Sars-CoV-2 envelope and membrane proteins: structural differences linked to virus characteristics? BioMed Res Int 2020;2020:1–6. https://doi.org/10.1155/2020/4389089.

[17] Becerra-Flores M, Cardozo T. SARS-CoV-2 viral spike G614 mutation exhibits higher case fatality rate. Int J Clin Pract 2020;74:e13525. https://doi.org/10.1111/ijcp.13525.

[18] Biswas A, Bhattacharjee U, Chakrabarti AK, Tewari DN, Banu H, Dutta S. Emergence of Novel Coronavirus and COVID-19: whether to stay or die out? Crit Rev Microbiol 2020:1–12. https://doi.org/10.1080/1040841X.2020.1739001. 0.

[19] Bzówka M, Mitusińska K, Raczyńska A, Samol A, Tuszyński JA, Góra A. Structural and evolutionary analysis indicate that the SARS-CoV-2 mpro is a challenging target for small-molecule inhibitor design. Int J Mol Sci 2020;21. https://doi.org/10.3390/ijms21093099.

[20] Elbe S, Buckland-Merrett G. Data, disease and diplomacy: GISAID's innovative contribution to global health. Glob Chall 2017;1:33–46. https://doi.org/10.1002/gch2.1018.

[21] Berman HM, Westbrook J, Feng Z, Gilliland G, Bhat TN, Weissig H, et al. The protein data bank. Nucleic Acids Res 2000;28:235–42.

[22] Roy A, Kucukural A, Zhang Y. I-TASSER: a unified platform for automated protein structure and function prediction. Nat Protoc 2010;5:725–38.

[23] Zhang Y. I-TASSER server for protein 3D structure prediction. BMC Bioinf 2008;9. https://doi.org/10.1186/1471-2105-9-40. 40–40.

[24] Rodrigues CH, Pires DE, Ascher DB. DynaMut: predicting the impact of mutations on protein conformation, flexibility and stability. Nucleic Acids Res 2018;46. https://doi.org/10.1093/nar/gky300. W350–5.

[25] Baby K, Maity S, Mehta CH, Suresh A, Nayak UY, Nayak Y. Targeting SARS-CoV-2 RNA-dependent RNA polymerase: an in silico drug repurposing for COVID-19. F1000Research 2020;9:1166. https://doi.org/10.12688/f1000research.26359.1.

[26] Bowers KJ, Chow DE, Xu H, Dror RO, Eastwood MP, Gregersen BA, et al. Scalable algorithms for molecular dynamics simulations on commodity clusters. SC 06 Proc. 2006 ACMIEEE Conf. Supercomput. 2006. https://doi.org/10.1109/SC.2006.54. 43–43.

[27] Sugita Y, Kitao A. Dependence of protein stability on the structure of the denatured state: free energy calculations of I56V mutation in human lysozyme. Biophys J 1998;75:2178–87.

[28] Balsera MA, Wriggers W, Oono Y, Schulten K. Principal component analysis and long time protein dynamics. J Phys Chem 1996;100:2567–72. https://doi.org/10.1021/jp9536920.

[29] Sittel F, Jain A, Stock G. Principal component analysis of molecular dynamics: on the use of Cartesian vs. internal coordinates. J Chem Phys 2014;141:014111. https://doi.org/10.1063/1.4885338.

[30] Ernst M, Sittel F, Stock G. Contact- and distance-based principal component analysis of protein dynamics. J Chem Phys 2015;143:244114. https://doi.org/10.1063/1.4938249.

[31] Kume A, Kawai S, Kato R, Iwata S, Shimizu K, Honda H. Exploring high-affinity binding properties of octamer peptides by principal component analysis of tetramer peptides. J Biosci Bioeng 2017;123:230–8. https://doi.org/10.1016/j.jbiosc.2016.08.005.

[32] Ouaray Z, ElSawy KM, Lane DP, Essex JW, Verma C. Reactivation of mutant p53: constraints on mechanism highlighted by principal component analysis of the DNA binding domain. Proteins 2016;84:1443–61. https://doi.org/10.1002/prot.25089.

[33] Iida S, Mashimo T, Kurosawa T, Hojo H, Muta H, Goto Y, et al. Variation of free-energy landscape of the p53 C-terminal domain induced by acetylation: enhanced conformational sampling. J Comput Chem 2016;37:2687–700. https://doi.org/10.1002/jcc.24494.

[34] Tripathi S, Srivastava G, Sharma A. Molecular dynamics simulation and free energy landscape methods in probing L215H, L217R and L225M βI-tubulin mutations causing paclitaxel resistance in cancer cells. Biochem Biophys Res Commun 2016; 476:273–9. https://doi.org/10.1016/j.bbrc.2016.05.112.

[35] Martis EAF, Coutinho EC. Free energy-based methods to understand drug resistance mutations. In: Mohan CG, editor. Struct. Bioinforma. Appl. Preclin. Drug discov. Process. Cham: Springer International Publishing; 2019. p. 1–24. https://doi.org/10.1007/978-3-030-05282-9_1.

[36] Sohaib Shahzan M, Smiline Girija AS, Vijayashree Priyadharsini J. A computational study targeting the mutated L321F of ERG11 gene in C. albicans, associated with fluconazole resistance with bioactive compounds from Acacia nilotica. J Mycol Médicale 2019:100899. https://doi.org/10.1016/j.mycmed.2019.100899.

[37] Rajendran V, Gopalakrishnan C, Sethumadhavan R. Pathological role of a point mutation (T315I) in BCR-ABL1 protein—a computational insight. J Cell Biochem 2018;119:918–25. https://doi.org/10.1002/jcb.26257.

[38] Hassan SkS, Choudhury PP, Roy B. SARS-CoV2 envelope protein: non-synonymous mutations and its consequences. Genomics 2020;112:3890–2. https://doi.org/10.1016/j.ygeno.2020.07.001.

[40] Liu X, Fuentes EJ. Emerging themes in PDZ domain signaling. Int Rev Cell Mol Biol 2019;343:129–218. https://doi.org/10.1016/bs.ircmb.2018.05.013.

[43] Rahman MS, Hoque MN, Islam MR, Islam I, Mishu ID, Rahaman MdM, et al. Mutational insights into the envelope protein of SARS-CoV-2. Gene Rep 2021;22: 100997. https://doi.org/10.1016/j.genrep.2020.100997.

[44] Ye Y, Hogue BG. Role of the coronavirus E viroporin protein transmembrane domain in virus assembly. J Virol 2007;81:3597–607. https://doi.org/10.1128/JVI.01472-06.

[45] Liu X, Shi D, Zhou S, Liu H, Liu H, Yao X. Molecular dynamics simulations and novel drug discovery. Expet Opin Drug Discov 2018;13:23–37. https://doi.org/10.1080/17460441.2018.1403419.

[46] Liu H, Yao X. Molecular basis of the interaction for an essential subunit PA-PB1 in influenza virus RNA polymerase: insights from molecular dynamics simulation and free energy calculation. Mol Pharm 2010;7:75–85. https://doi.org/10.1021/mp900131p.

[47] He M, Li W, Zheng Q, Zhang H. A molecular dynamics investigation into the mechanisms of alectinib resistance of three ALK mutants. J Cell Biochem 2018;119: 5332–42. https://doi.org/10.1002/jcb.26666.

[48] Berhanu WM, Masunov AE. Molecular dynamic simulation of wild type and mutants of the polymorphic amyloid NNQNTF segments of elk prion: structural stability and thermodynamic of association. Biopolymers 2011;95:573–90. https://doi.org/10.1002/bip.21611.

[49] Chong S-H, Lee C, Kang G, Park M, Ham S. Structural and thermodynamic investigations on the aggregation and folding of acylphosphatase by molecular dynamics simulations and solvation free energy analysis. J Am Chem Soc 2011; 133:7075–83. https://doi.org/10.1021/ja1116233.

[50] Bavi R, Kumar R, Choi L, Lee KW. Exploration of novel inhibitors for bruton's tyrosine kinase by 3D QSAR modeling and molecular dynamics simulation. PloS One 2016;11:e0147190. https://doi.org/10.1371/journal.pone.0147190.

[51] Nagasundaram N, Zhu H, Liu J, V K, C GPD, Chakraborty C, et al. Analysing the effect of mutation on protein function and discovering potential inhibitors of CDK4: molecular modelling and dynamics studies. PloS One 2015;10. https://doi.org/10.1371/journal.pone.0133969.

[52] Lobanov MY, Bogatyreva NS, Galzitskaya OV. Radius of gyration as an indicator of protein structure compactness. Mol Biol 2008;42:623–8. https://doi.org/10.1134/S0026893308040195.

[53] Smilgies D-M, Folta-Stogniew E. Molecular weight–gyration radius relation of globular proteins: a comparison of light scattering, small-angle X-ray scattering and structure-based data. J Appl Crystallogr 2015;48:1604–6. https://doi.org/10.1107/S1600576715015551.

[54] Khan MT, Ali A, Wang Q, Irfan M, Khan A, Zeb MT, et al. Marine natural compounds as potents inhibitors against the main protease of SARS-CoV-2. A molecular dynamic study. J Biomol Struct Dyn 2020:1–14. https://doi.org/10.1080/07391102.2020.1769733. 0.

[55] Khan MT, Khan A, Rehman AU, Wang Y, Akhtar K, Malik SI, et al. Structural and free energy landscape of novel mutations in ribosomal protein S1 (rpsA) associated with pyrazinamide resistance. Sci Rep 2019;9:7482. https://doi.org/10.1038/s41598-019-44013-9.

[56] Gerlt JA, Kreevoy MM, Cleland W, Frey PA. Understanding enzymic catalysis: the importance of short, strong hydrogen bonds. Chem Biol 1997;4:259–67.

[57] Hubbard RE, Haider MK. Hydrogen bonds in proteins: role and strength. eLS. American Cancer Society; 2010. https://doi.org/10.1002/9780470015902.a0003011.pub2.

[58] Pace CN, Fu H, Fryar KL, Landua J, Trevino SR, Schell D, et al. Contribution of hydrogen bonds to protein stability. Protein Sci Publ Protein Soc 2014;23:652–61. https://doi.org/10.1002/pro.2449.

[59] Mukherjee J, Gupta MN. Increasing importance of protein flexibility in designing biocatalytic processes. Biotechnol Rep 2015;6:119–23. https://doi.org/10.1016/j.btre.2015.04.001.

[60] Yang F, Zheng G, Fu T, Li X, Tu G, Li YH, et al. Prediction of the binding mode and resistance profile for a dual-target pyrrolyl diketo acid scaffold against HIV-1 integrase and reverse-transcriptase-associated ribonuclease H. Phys Chem Chem Phys 2018;20:23873–84. https://doi.org/10.1039/C8CP01843J.

[61] Junaid M, Khan MT, Malik SI, Wei D-Q. Insights into the mechanisms of pyrazinamide resistance of three pyrazinamidase mutants N11K, P69T and D126N. J Chem Inf Model 2018. https://doi.org/10.1021/acs.jcim.8b00525.

[62] Khan MT, Ali S, Zeb MT, Kaushik AC, Malik SI, Wei D-Q. Gibbs free energy calculation of mutation in PncA and RpsA associated with pyrazinamide resistance. Front Mol Biosci 2020;7. https://doi.org/10.3389/fmolb.2020.00052.